

## Supporting Information

Enhanced visible light photocatalytic activity in  
BiOCl/SnO<sub>2</sub>: heterojunction of two wide band-gap  
semiconductors

Menglin Sun, Qihang Zhao, Chunfang Du\*, and Zhiliang Liu\*

*College of Chemistry and Chemical Engineering, Inner Mongolia University, Hohhot,  
Inner Mongolia 010021, P. R. China*

Table S1 The results of each deconvoluted component of BiOCl, SnO<sub>2</sub> and 0.5BiOCl/SnO<sub>2</sub> composite

Samples	Bi 4 <i>f</i> (eV)		Sn 3 <i>d</i> (eV)		Cl 2 <i>p</i> (eV)		O 1 <i>s</i> (eV)		
	4 <i>f</i> <sub>5/2</sub>	4 <i>f</i> <sub>7/2</sub>	3 <i>d</i> <sub>3/2</sub>	3 <i>d</i> <sub>5/2</sub>	2 <i>p</i> <sub>1/2</sub>	2 <i>p</i> <sub>3/2</sub>			
BiOCl	43.8%	56.2%	-	-	41.5%	58.5%	11.3%	25.0%	63.7%
SnO <sub>2</sub>	-	-	41.9%	58.1%	-	-	16.1%	28.0%	55.9%
0.5BiOCl/SnO <sub>2</sub>	42.5%	57.5%	42.5%	57.5%	42.3%	57.7%	32.8%	38.2%	29.0%

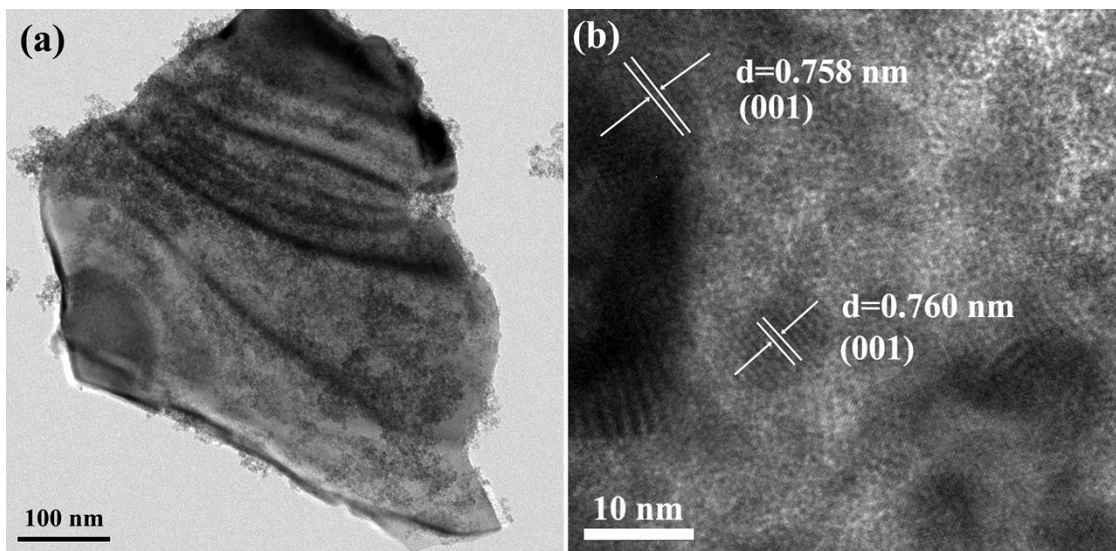


Fig.S1 TEM and HRTEM images of 0.5BiOCl/SnO<sub>2</sub>

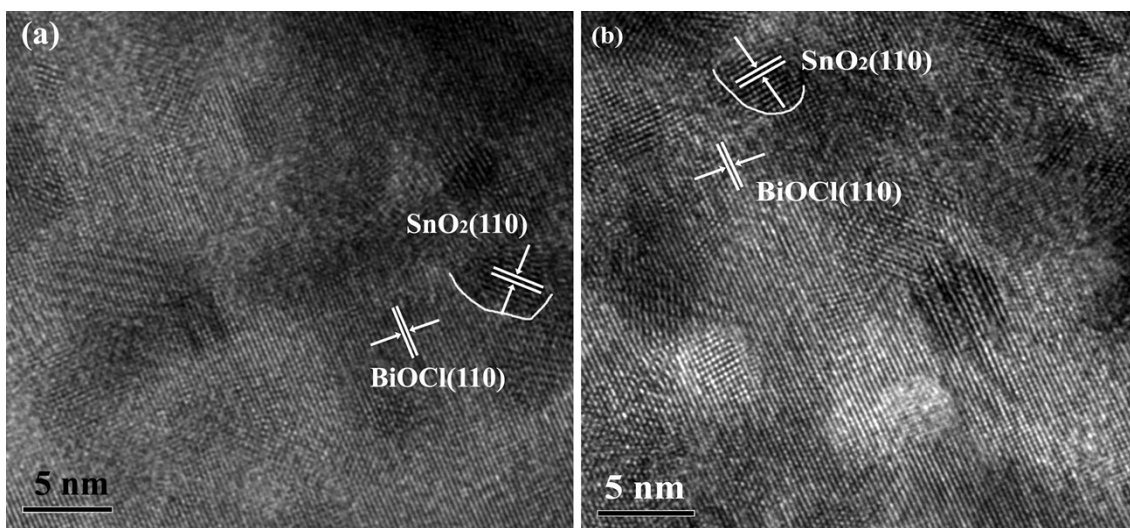


Fig.S2 HRTEM images of 0.5BiOCl/SnO<sub>2</sub>

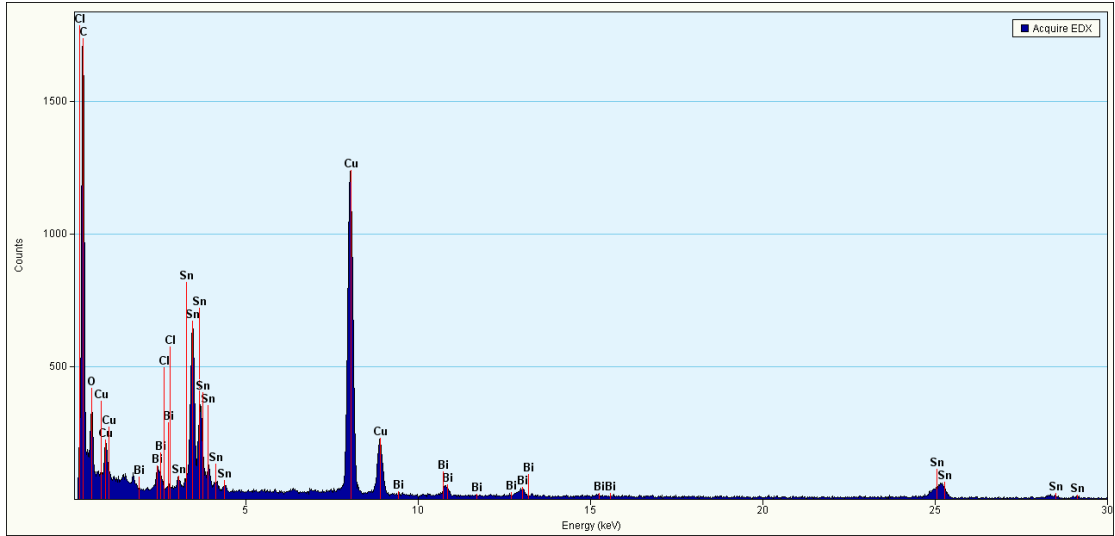


Fig. S3. EDS spectrum of 0.5BiOCl/SnO<sub>2</sub> composite.

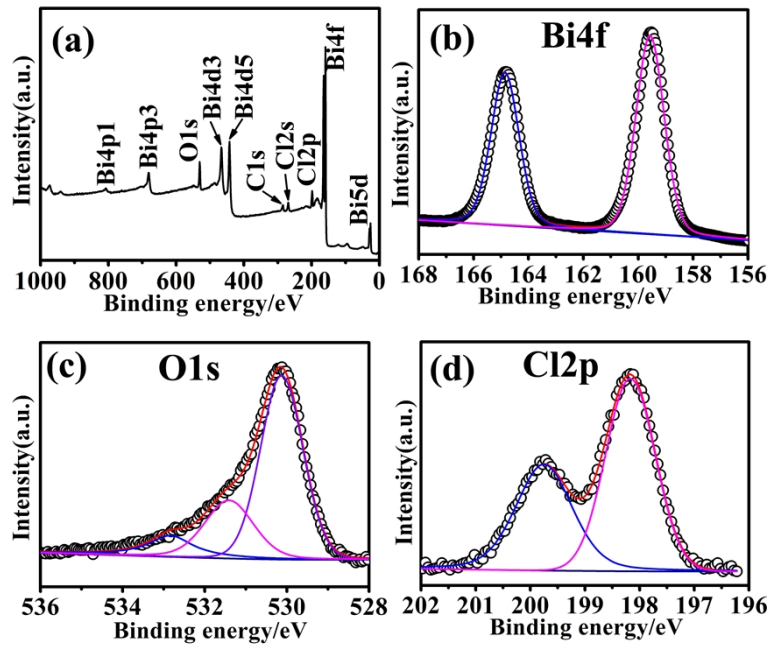


Fig. S4. XPS spectra of pure BiOCl: survey scan (a), Bi 4f (b), O1s (c) and Cl 2p (d).

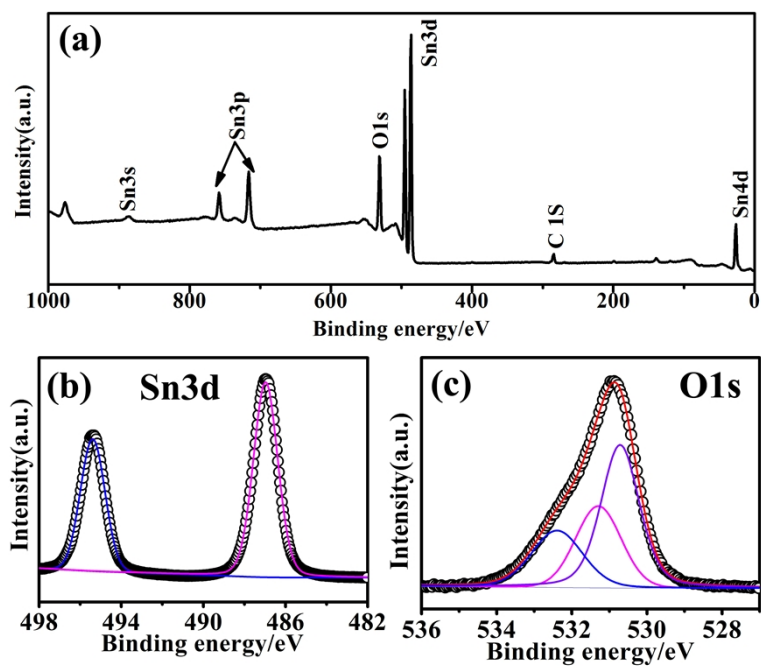


Fig. S5. XPS spectra of pure SnO<sub>2</sub>: survey scan (a), Sn3d (b) and O1s (c).

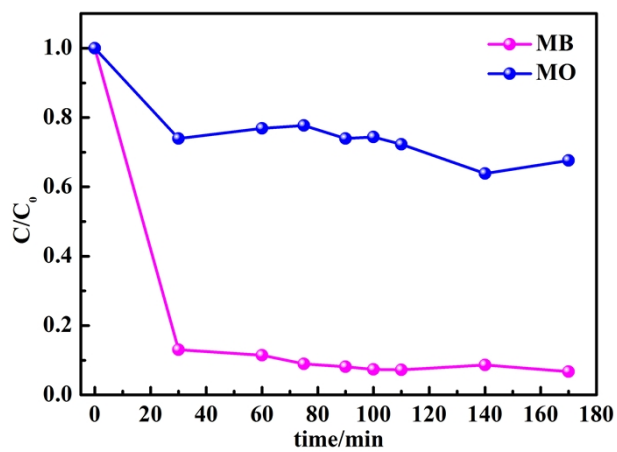


Fig. S6. The adsorption behavior of BiOCl for ionic methyl orange (MO) and cationic methyl blue (MB).

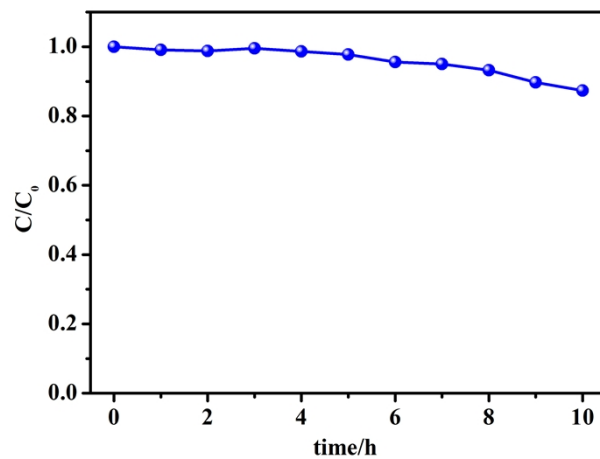


Fig. S7. The photodegradation of RhB without any catalyst under visible light irradiation.

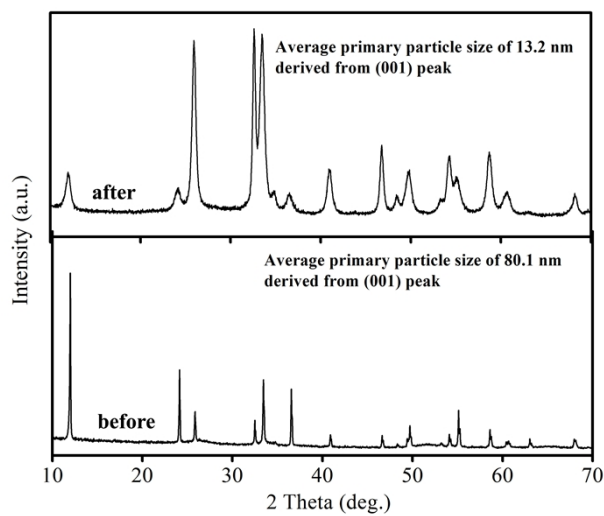


Fig. S8 The XRD patterns of 0.5BiOCl/SnO<sub>2</sub> before and after degradation for 8 h

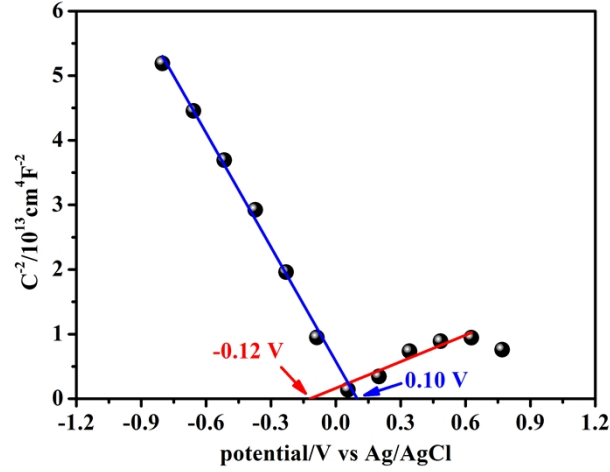


Fig.S9 Mott-Schottky plots of 0.5BiOCl/SnO<sub>2</sub>

The p-type and n-type characteristics of the semiconductors can be deduced from Mott-Schottky plots and equations as follows:<sup>1</sup>

$$\frac{1}{C^2} = \frac{2}{e\epsilon\epsilon_0 N_A} \left( E - E_{fb} - \frac{kT}{e} \right) \text{ for n-type semiconductor} \quad (1)$$

$$\frac{1}{C^2} = \frac{2}{e\epsilon\epsilon_0 N_D} \left( -E + E_{fb} - \frac{kT}{e} \right) \text{ for p-type semiconductor} \quad (2)$$

Where  $\epsilon_0$  is the permittivity of vacuum ( $8.854 \times 10^{-12}$  F/m),  $\epsilon$  is the dielectric constant of SnO<sub>2</sub> ( $\epsilon=14$ ) and BiOCl ( $\epsilon=5.59$ ), and  $e$  is the electronic charge ( $1.603 \times 10^{-19}$  C).  $N_D$  and  $N_A$  are the donor and acceptor densities, respectively, which are calculated from the slope of the fitting curves.  $T$  is the operation temperature (298 K), and  $k$  is Boltzmann's constant ( $1.38 \times 10^{-23}$  J/K).  $E$  is the electrode potential,  $E_{fb}$  is the flat-band potential, and  $C$  is the depletion-layer capacitance.

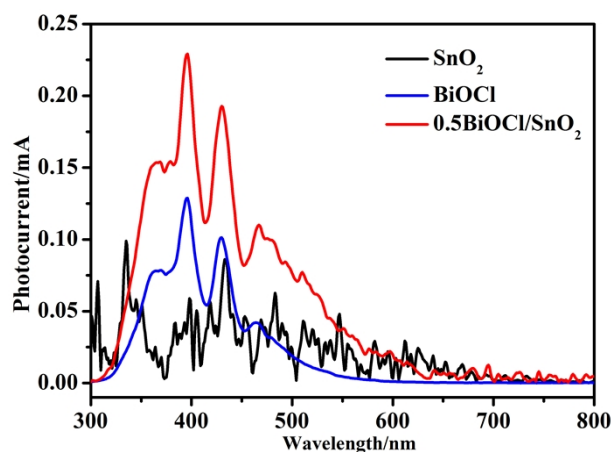


Fig. S10. The SPC spectra of pure BiOCl, SnO<sub>2</sub> and 0.5BiOCl/SnO<sub>2</sub> composite.

The surface photovoltage (SPV) technique is a rapid and effective method to study the photovoltaic properties of semiconductor photocatalysts. It always is used to investigate the transfer behavior of photo-induced charge carriers with high sensitivity to defect states at surface, bulk or any buried interface in the synthesized products.<sup>2</sup> Whenever the photo-induced charge carriers are separated, a photovoltage signal arises. Thus, the fundamental properties of the light absorption and the transport of excess carriers in the semiconductors decides the production of a SPV signal.<sup>3,4</sup> That means the type of semiconductors (p-type or n-type), band-gap energy and gap states could be deduced from the SPV signals.<sup>5</sup> A positive SPV signal indicates the photo-induced holes immigrate to the irradiation side of the product, and a negative SPV signal suggests that the photo-induced electrons move to the irradiation side. Furthermore, the threshold of the SPV response of semiconductors is generally consistent with the optical absorption.<sup>6</sup>

The SPV and SPC response intensities mostly depend on the charge separation efficiency. A higher separation efficiency of photo-induced charges would display a

stronger SPV response intensity.<sup>7</sup> The efficient separation of photo-induced electron-hole pairs could prolong the lifetime of the charge carriers and improve the efficiency of the interfacial charge transfer to adsorbed substrates and then contributes to the higher photocatalytic activity of photocatalysts.<sup>8</sup>

When checking the SPV signals together with the corresponding phase spectrum, the detailed transfer direction and separation-recombination process of the photo-induced charge carriers could be deduced. Taking Cu<sub>2</sub>O and ZnO films as an example,<sup>6</sup> the phase value of Cu<sub>2</sub>O film is about -140° and keep this value during the whole SPV response region, which indicates that negative charge accumulates at the surface of Cu<sub>2</sub>O film. However, the phase value of ZnO film is about 20°, which suggests that the positive charge accumulates at the surface of ZnO film.

## References

1. Y. Liu, Y. X. Yu, W. D. Zhang, *J. Phys. Chem. C*, 2013, **117**, 12949.
2. H. Fan, T. Jiang, H. Li, D. Wang, L. Wang, J. Zhai, D. He, P. Wang, T. Xie, *J. Phys. Chem. C*, 2011, **116**, 2425.
3. T. F. Xie, D. J. Wang, L. J. Zhu, C. Wang, T. J. Li, X. Q. Zhou, M. J. Wang, *J. Phys. Chem. B*, 2000, **104**, 8177.
4. F. A. Frame, T. K. Townsend, R. L. Chamousis, E. M. Sabio, T. Dittrich, N. D. Browning, F. E. Osterloh, *J. Am. Chem. Soc.*, 2011, **133**, 7264.
5. L. Chen, S. Li, Z. Liu, Y. Lu, D. Wang, Y. Lin, T. Xie, *Phys. Chem. Chem. Phys.*, 2013, **15**, 14262.

6. T. Jiang, T. Xie, Y. Zhang, L. Chen, L. Peng, H. Li, D. Wang, *Phys. Chem. Chem. Phys.*, 2010, **12**, 15476.
7. H. Fan, H. Li, B. Liu, Y. Lu, T. Xie, D. Wang, *ACS Appl. Mater. Interfaces*, 2012, **4**, 4853.
8. Z. Zhang, C. Shao, X. Li, C. Wang, M. Zhang, Y. Liu, *ACS Appl. Mater. Interfaces*, 2010, **2**, 2915.